Earth and Planetary Science Letters 365 (2013) 243–252

Contents lists available at SciVerse ScienceDirect

Earth and Planetary Science Letters

journal homepage: www.elsevier.com/locate/epsl

Increasing chemical weathering in the Himalayan system since the Last Glacial Maximum

Maarten Lupker [a,*], Christian France-Lanord [a], Valier Galy [b], Jérôme Lavé [a], Hermann Kudrass [c]

[a] Centre de Recherches Pétrographiques et Géochimiques (CRPG), UMR 7358, CNRS-Université de Lorraine, 15 rue Notre Dame des Pauvres, 54501 Vandoeuvre les Nancy, Cedex, France
[b] Woods Hole Oceanographic Institution (WHOI)—Department of Marine Chemistry and Geochemistry, 360 Woods Hole Rd., Woods Hole, MA 02543, USA
[c] MARUM zentrum für Marine Umweltwissenschaften, Bremen, Germany

ARTICLE INFO

Article history:
Received 25 September 2012
Received in revised form
25 January 2013
Accepted 28 January 2013
Editor: T.M. Harrison

Keywords:
Himalayan system
chemical weathering
Last Glacial Maximum
source to sink

ABSTRACT

Continental chemical weathering is central in Earth's surface biogeochemical cycles as it redistributes elements across reservoirs such as the crust and the oceans. However the evolution of weathering through time and its response to external forcing such as changes in climate remain poorly constrained. In this work, a composite sediment record from the Bay of Bengal is used to document the evolution of chemical weathering in the Himalayan system (Himalayan range and Indo-Gangetic floodplain), the world largest sediment conveyor to the oceans, since the Last Glacial Maximum (LGM). The degree of weathering of the sediments is documented using mobile to immobile ratios such as K/Si and H_2O^+/Si as well as detrital calcite abundance. Robust weathering proxies are derived by correcting the chemical composition of sediment for sorting effects that occur during transport and deposition. The Bay of Bengal record is also further compared to the chemical composition of modern river sediments from the Ganga and Brahmaputra basin. Weathering proxies all indicate that the sediments exported by the Ganga and Brahmaputra Rivers became increasingly weathered over the past ~21 kyr, whereas, Sr, Nd and major elements suggest a constant sediment provenance in the system over the last 21 kyr. These changes in the degree of weathering of the sediments show that the weathering flux exported by the system to the Indian Ocean during the LGM was significantly lower than at present and demonstrate that chemical weathering in continental scale basins such as the Ganga and Brahmaputra responds to Late Quaternary climate changes.

1. Introduction

Chemical weathering of continental rocks is the main source of soluble elements to the oceans and therefore exerts a first order control on oceanic bio-geochemical cycles. Over geologic time scales, silicate weathering and subsequent carbonate precipitation also draws down atmospheric CO_2 thereby stabilizing the earth's climate (Walker et al., 1981). Continental weathering fluxes are a function of continent lithology, tectonic activity and climate but the mechanisms and feedbacks linking silicate weathering to the earth's climate remain debated (France-Lanord and Derry, 1997; Willenbring and von Blanckenburg, 2011). A better understanding of these complex climate-weathering couplings can be gained by studying the response of continents to climatic transitions in the past.

The role of the Himalayan orogeny in the long-term forcing of oceanic cycles and the global climate has retained much attention (e.g. Raymo et al., 1988; France-Lanord and Derry, 1997). However, the temporal variability of and controls on the evolution of weathering fluxes exported by large basins remains poorly constrained and is often difficult to reconstruct (Limmer et al., 2012). In particular, direct characterization of the response of chemical weathering to abrupt climate perturbations has heretofore remained a challenge. We present a record of chemical weathering intensity in the Himalayan system since the LGM. The Himalayan system is defined here as the Himalayan range and the downstream Indo-Gangetic floodplain drained by Ganga and Brahmaputra Rivers. No major change in tectonic forcing of the Himalayan orogeny has been documented so far over the last glacial–interglacial period, which enables us to discuss variations in sediment weathering as a response to climate change.

2. Setting and methods

The central part of the Himalayan range is drained by two major rivers, the Ganga and Brahmaputra (Fig. 1). Currently, the Ganga and Brahmaputra transfers ca. 1×10^9 Mt of sediments to

* Correspondence to: IGP-ETHZ, NW C 85, Clausiusstrasse 25, 8092 Zürich, Switzerland. Tel.: +41 446 329 383.
E-mail address: maarten.lupker@erdw.ethz.ch (M. Lupker).

0012-821X/$ - see front matter © 2013 Elsevier B.V. All rights reserved.
http://dx.doi.org/10.1016/j.epsl.2013.01.038

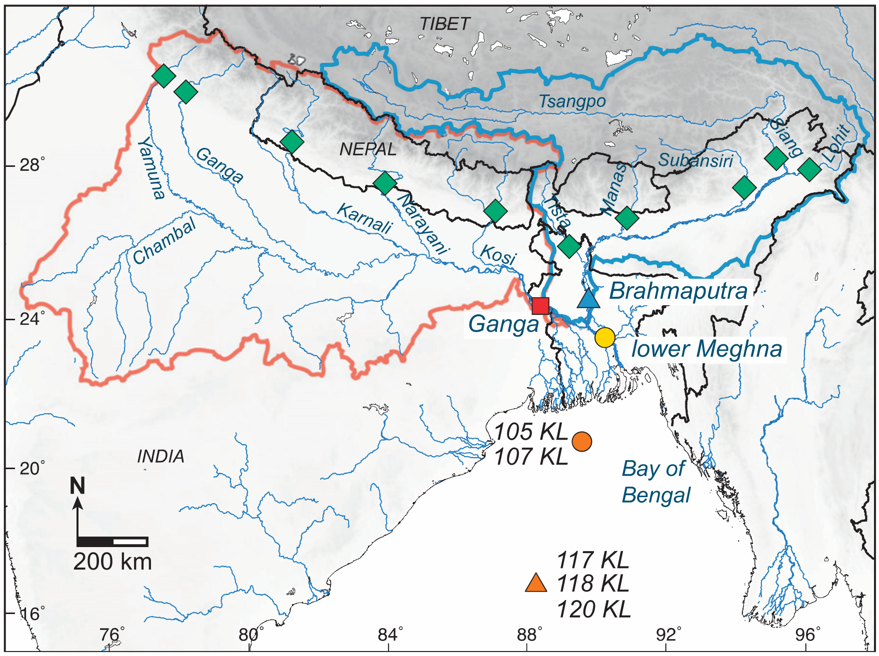

Fig. 1. Geographical setting of the Himalayan system. Modern river sediments were sampled in the Ganga and Brahmaputra basin at the Himalayan front (green diamonds), at the outlet of the Ganga basin (red square) and the Brahmaputra basin (blue triangle) and finally after their confluence in the lower Meghna (yellow circle). These sediments were compared to the sediment record of the Bay of Bengal that represents a composite record from proximal shelf sediments (105 KL and 107 KL) and from the middle fan channel levees (117 KL, 118 KL and 120 KL). (For interpretation of the references to color in this figure legend, the reader is referred to the web version of this article.)

the Bay of Bengal, of which 90% is transported during the monsoon (RSP, 1996). River sediments were sampled mainly during monsoon seasons, in 2002, 2004, 2005, 2007, 2008 and 2010 across the Indo-Gangetic floodplain. Sampling locations mainly included the front of the Himalayan range for the main trans-Himalayan Rivers of the Ganga and Brahmaputra system, the outlet of the Ganga and the Brahmaputra as well as their confluence – the lower Meghna – which integrates the entire sediment load exported from the Ganga and Brahmaputra basin (Fig. 1). When possible, sediments were sampled along vertical depth profiles through the water column in order to capture the full variability of the sediment load. These profiles were complemented by bedload samples dredged from the active channel of the rivers and freshly exposed bar sediments. Details on the sampling procedure are described in Lupker et al. (2011).

Sediment cores were retrieved during RV *Sonne* cruise SO93 in 1994 from the shelf (105 KL and 107 KL) and the active channel levee system of the middle fan (117 KL, 118 KL and 120 KL) (Ittekkot et al., 2003). The chronology of the cores is provided by re-calibrated (Reimer et al., 2009) ^{14}C ages on planktonic foraminifers (Weber et al., 1997) as well as ^{137}Cs, ^{210}Pb and ^{228}Ra gamma spectrometry (Michels et al., 1998). Scarce hemipelagic layers were excluded from the study in order to focus on turbiditic sediments representing the Ganga and Brahmaputra detrital signal (Pierson-Wickmann et al., 2001; Weber et al., 1997). We interpret our data by constructing a composite Log from the shelf and levees core following the approach detailed in Galy et al. (2008).

Suspended river sediments were filtered through 0.22 μm PES membrane filters within 24 h of sampling and dried in the lab. Major element concentration was determined by ICP-OES after $LiBO_2$ fusion at SARM, Nancy – France (Carignan et al., 2001). Core samples were repeatedly rinsed with water in order to remove salt contributions. Nevertheless, Na was not considered in this study due to seawater contamination even after these rinsing steps. Carbonate contents were measured manometrically from the CO_2 released after reaction with H_3PO_4 and the evolved CO_2 was subsequently analyzed for C and O isotopic composition (Galy et al., 1999). Sr and Nd isotopic compositions were measured on the acid leached, silicate fraction of the river and core sediments by TIMS after classical separation and purification by ion exchange resins. Sediment hydration [H_2O^+] and isotopic composition δD-SMOW was measured by EA-IRMS after degassing the samples to remove adsorbed free-water (Lupker et al., 2012a). The long-term reproducibility is better than 0.1H_2O^+ wt% and 2‰ δD-SMOW.

3. Sediment sorting effects on the chemical composition of detrital sediments

3.1. Hydrodynamic control of sediment sorting

The chemical composition of river sediments has to be interpreted carefully. Sediment vertical depth profiles recovered from the water column of large rivers show a strong heterogeneity in terms of concentration and chemical composition. These heterogeneities are the result of the hydrodynamic sorting of sediments, based on grain-size, shape and density, which induce mineralogical and thus chemical differentiation of sediments within the water column (Bouchez et al., 2011a, 2011b; Garzanti et al., 2011; Lupker et al., 2011; Singh and France-Lanord, 2002). The mineralogy of sediments from the Himalayan system is dominated by quartz, micas and feldspar, with occurrences of other phyllosilicates, clay assemblages and hydroxides in the finer fraction (Garzanti et al., 2010, 2011). These minerals are segregated during sediment transport: coarse-grained quartz is enriched in the bedload and at the bottom of the water column while phyllosilicates such as micas and clays are comparatively enriched in the shallow surface waters of the river, leading to a strong contrast in chemical composition between samples of a single reach. This is best illustrated using the immobile element ratios Fe/Si and Al/Si (Fig. 2).

Fe, Al and Si are, to a first order, immobile elements during Himalayan erosion and are thus not notably affected by chemical weathering (Galy and France-Lanord, 2001). The sediments sampled across the Indo-Gangetic plain form a unique mixing trend (to the exception of a few bedload samples that are enriched in Fe due to heavy mineral placer effects) between quartz rich (low Al/Si and Fe/Si) bottom sediments and clay rich (high Al/Si and Fe/Si) surface sediments. Al/Si and Fe/Si are directly correlated to the bulk sediment grain-size and are a proxy of mineral sorting (Bouchez et al., 2011a; Lupker et al., 2011). A single sediment sample from a given river reach can therefore not be considered, a priori, as representative of the whole sediment load, its chemical composition being dependent on river hydrodynamics at the moment of sampling.

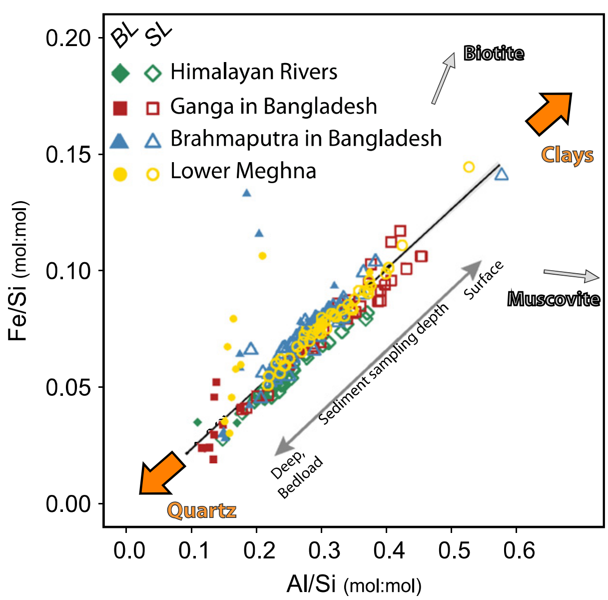

Fig. 2. Hydraulic sorting effect on the Si–Al–Fe chemical composition of sediments. Suspended sediments are the result of the mixing between a low Al/Si and Fe/Si quartz-rich coarse-grained end-member and a high Al/Si and Fe/Si surface end-member relatively enriched in phylosilicates.

3.2. Weathering proxies in modern river sediments

The degree of chemical weathering experienced by sediments in the Himalayan system can be traced from detrital sediments by using the mobile to immobile elemental ratios of river sediments such as K/Si and H_2O^+/Si. The structural hydroxyl content of sediments, H_2O^+, is a proxy of chemical weathering that traces mineral hydrolysis and secondary neo-formations (Lupker et al., 2012a). Sediment sorting effects also apply to mobile elements such as K and H_2O^+. The K/Si and H_2O^+/Si ratios are dominantly controlled by the grain size of the sediments, i.e. clay to quartz mixing (Lupker et al., 2012a) and are, to a first order, linearly correlated to their Al/Si ratio as shown by Fig. 3, where these ratios are plotted for sediments from the modern Himalayan system. By using a sediment depth profile sampling approach on modern rivers, we characterize these sorting effects as this method allows sampling a full set of sediments covering a wide range of grain sizes. The degree of chemical weathering can then be assessed based on the trend formed by the chemical composition of the sediments in diagrams such as Fig. 3, this trend being representative of the entire sediment load exported by the considered river.

In addition to silicate weathering proxies, we determined the calcite content and the Ca/Si ratio in Bay of Bengal sediments that reflects the carbonate weathering intensity in the Himalayan system. Carbonates, including calcite, account for over 80% of the bulk Ca and Ca/Si therefore mainly reflects carbonate content. Both carbonates and Ca content are not grain size dependent (Lupker et al., 2011) and are therefore not corrected for sediment sorting.

3.3. Accounting for sediment sorting effects in detrital records

For detrital records such as the Bay of Bengal cores, changes in sediment transport and deposition patterns induce changes in the grain size of deposited sediments that, in turn, affect the chemical composition of the record. Hence, sediment sorting also has to be taken into account in order to compare the degree of weathering of samples with variable grain-sizes (variable Al/Si ratios). However, unlike for modern rivers, it is not possible for a given age interval of the record to recover a set of sediment samples spanning different grain sizes that would fully describe the

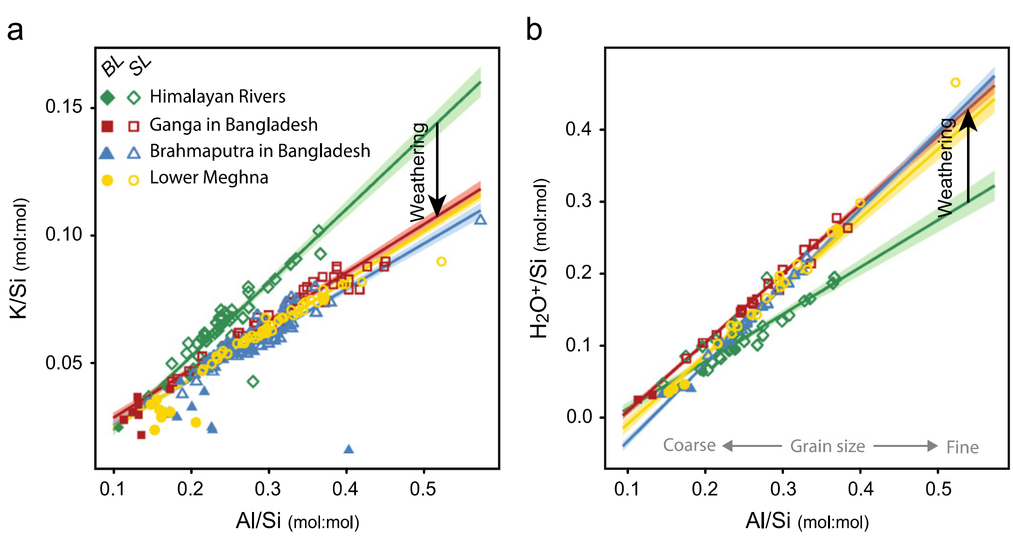

Fig. 3. Evolution of K/Si (a) and H_2O^+/Si (b) in the modern Himalayan system for river suspended load (SL) and bedload or bar sediments (BL). The transfer of sediments from the Himalayan front Rivers (green) to the outlet of the Ganga (red) and Brahmaputra (blue), as well as their confluence the lower-Meghna (yellow) results in a loss of K and an increase in H_2O^+ as weathering proceeds. Envelopes represent 0.95 confidence level on the linear regression. (For interpretation of the references to color in this figure legend, the reader is referred to the web version of this article.)

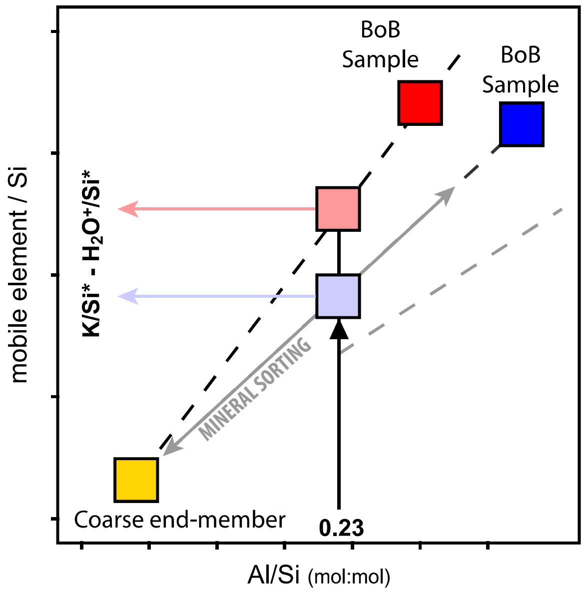

Fig. 4. Normalization of the chemical composition of sediments in of the Bay of Bengal record for hydraulic sorting effects. The K/Si and H_2O^+/Si ratios of the sample are normalized to a common Al/Si ratio of 0.23 assuming that the sediment sorting line passes through a unique coarse-grained end-member with a composition close to river bedloads (given in the Supplementary information, Table S1).

sediment weathering trend. By considering that each sample of the Bay of Bengal record is the result of the mixing between a coarse-grained end-member, similar to bedload material and a fine-grained, clay rich sediment, it is nevertheless possible to normalize mobile to immobile ratios ($\overline{X/Si}$) to a common Al/Si composition as illustrated in Fig. 4 and Eq. (1):

$$\frac{X^*}{Si} = \frac{\overline{Al}}{Si} \cdot A + B \quad (1)$$

where *A* and *B* are respectively the slope and intercept of the linear regression through the sample and coarse grained end-member composition (Fig. 4). Such normalized ratios allow comparing the chemical composition of sediments that have contrasted grain sizes, while properly accounting for sorting effects. Doing so, we assume that a unique coarse-grained end-member composition can be assigned to the low Al/Si mixing end-member and that the weathering signature is mainly carried by the small grain size, clay fraction of the sediment load. This is a reasonable approximation as: (1) contrary to the fine grained suspended load, no systematic evolution of K/Si and H_2O^+/Si ratios of modern bedloads in the Ganga basin is detected from up to downstream (Lupker et al., 2012a), suggesting that the effect of chemical weathering during transfer in the floodplain is negligible for the coarse fraction of the transported sediments, and (2) the transfer time of bedload material is thought to be an order of magnitude longer than that of fine-grained suspended load (Granet et al., 2010), which makes it less sensitive than the suspended load to short-term upstream variations.

All corrected ratios presented here were normalized to a common Al/Si value of 0.23. They are referred to as $\overline{X/Si}$ and are listed in the supplementary information along with the composition of the coarse grained end-member used in the calculations. The Al/Si value of 0.23 was chosen as the average composition of the sediments exported by the modern Ganga, which was determined by modeling the chemical composition of sediments as a function of the river's hydrological conditions and integrated over a 25-year average hydrograph (Lupker et al., 2011). This composition is also close to the composition of the Himalayan crust eroded in the Ganga basin (Lupker et al., 2011). It should be noted that the choice of the Al/Si ratio used for normalizing K/Si and H_2O^+/Si ratios only determines the absolute values of K/Si* and H_2O^+/Si* but has no influence on the general trends observed for Bay of Bengal sediments.

Before normalization, the raw K/Si and H_2O^+/Si ratios of sediments from the Bay of Bengal cores are correlated to Al/Si (Fig. 5), which supports that K/Si and H_2O^+/Si are dominantly controlled by grain size and sorting effects. However the normalized K/Si* and H_2O^+/Si* ratios show no correlation with Al/Si, which suggests that our normalization properly accounts for sediment sorting.

3.4. Comparison with modern river sediments

In order to compare the weathering degree of the Bay of Bengal sediment record to modern river sediments we applied a similar normalization to the river sediments. The average compositions of modern river sediments for elements prone to sorting effects (K/Si*, H_2O^+/Si*), reported in Fig. 5, were determined by evaluating the regression through all available data of each river reach and a coarse-grained end-member at Al/Si=0.23. The Himalayan front end-member was reconstructed from the river sediments sampled at the Himalayan front in the Ganga basin and the Brahmaputra basin separately assuming that ca. 60% of the total sediment flux exported to the Bay of Bengal come from the Brahmaputra and the remaining 40% come from the Ganga basin (RSP, 1996). For compositions that are not affected by sorting effects (calcite, Ca/Si, $^{87}Sr/^{86}Sr$, εNd, $\delta^{18}O$ and $\delta^{13}C$), a simple average for the Ganga, Brahmaputra and lower Meghna and a weighted mean for the Himalayan front were considered (details can be found in supplementary information and Table S2).

4. Weathering in the Himalayan system

4.1. Weathering in the modern system

Chemical weathering is marked by a change in the mobile to immobile ratio at constant Al/Si ratio. This mobile element depletion is highest for fine-grained (high Al/Si) sediments (Fig. 3). Modern Himalayan rivers sediments, sampled at the front of the range show high K/Si ratios and low H_2O^+/Si ratios compared to the sediments sampled at the outlet of the Ganga and Brahmaputra basins and their confluence, the lower Meghna (Fig. 3). The loss of K and gain in hydration during floodplain transfer marks the weathering of the sediments within the floodplain. Even if part of this weathering signal may stem from the sediment contribution of the southern (Ganga) and eastern (Brahmaputra) tributaries, their sediment fluxes remain small compared to that of Himalayan tributaries (Lupker et al., 2012a; Singh and France-Lanord, 2002). Calcite weathering in the modern floodplain is significant and leads to almost complete dissolution in Brahmaputra sediments in Bangladesh (Singh and France-Lanord, 2002; Singh et al., 2005) while modern Ganga sediments in Bangladesh display a low calcite content of ca. 3 wt% (Lupker et al., 2012a).

It has been shown that in the modern Ganga basin, weathering within the floodplain outweighs weathering within the Himalayan range (Lupker et al., 2012a; West et al., 2002). Significant *K* depletion and H_2O^+ gain is only recorded when sediments transit through the floodplain (Lupker et al., 2012a), which is attributed to the longer residence time of sediments in the floodplain than in the Himalayan range. Overall, these observations emphasize the strong floodplain control on weathering in the Himalayan system.

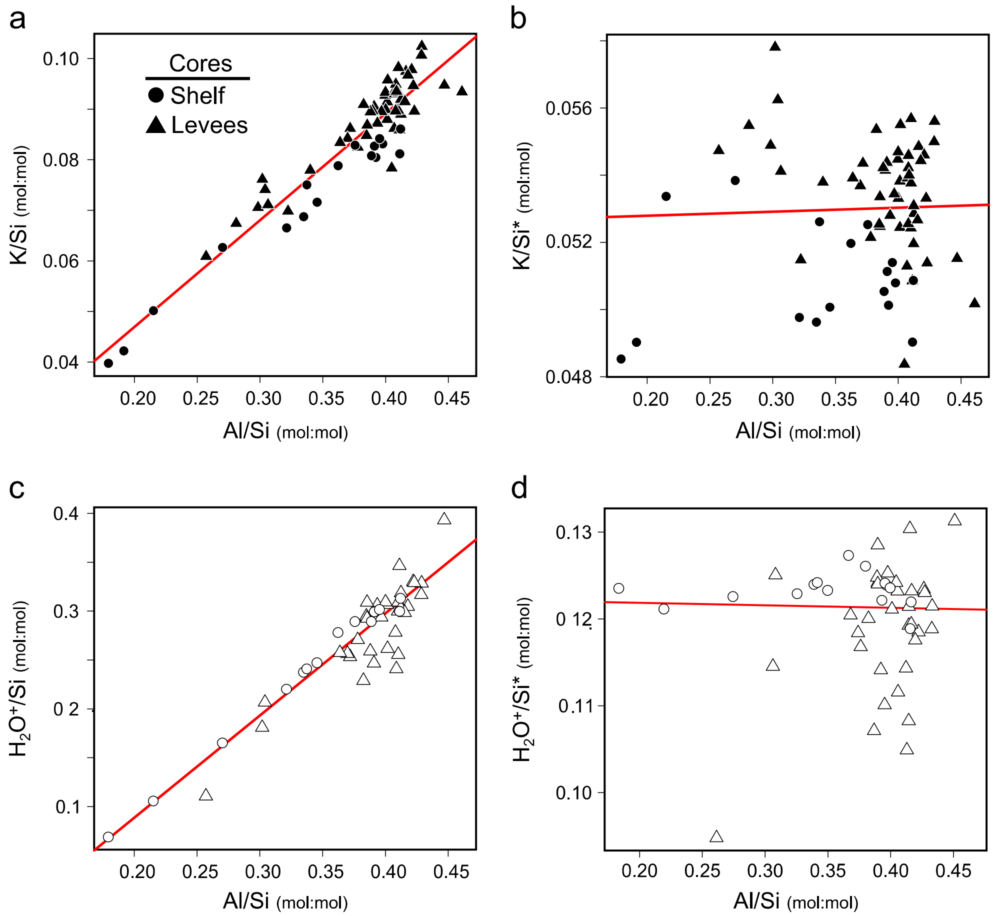

Fig. 5. K/Si and H_2O^+/Si in Bay of Bengal core sediments are strongly correlated to Al/Si, which is a proxy for grain size (Bouchez et al., 2011a; Lupker et al., 2011). Correction for hydraulic mineral sorting yields unbiased weathering indicators (K/Si* and H_2O^+/Si*).

4.2. *Weathering record of the Bay of Bengal*

The normalized weathering indexes (K/Si* and H_2O^+/Si*) are not biased by sorting effects and can thus be applied to the Bay of Bengal record to reconstruct temporal variations in chemical weathering. Composite logs of K/Si* and H_2O^+/Si* (Fig. 6) show a progressive evolution towards lower K/Si* and higher H_2O^+/Si* ratios from the LGM to present. Both weathering proxies suggest that during the LGM, sediments exported to the Bay of Bengal were less weathered than recent Bay of Bengal and modern lower-Meghna sediments. It should also be noted that the chemical composition of sediments from the most recent part of the Bay of Bengal record agrees well with that of the sediments currently exported by the lower Meghna (Fig. 6).

Calcite content and Ca/Si ratios also decrease from LGM to present (Fig. 6). Calcite in sediments from the Bay of Bengal is of detrital origin as demonstrated by their isotopic composition ($\delta^{18}O_{PDB}$ ranging from −15 to −6‰, see electronic appendix), much lower than marine biogenic calcite (Hoehndorf et al., 2003) and within the range of composition of detrital Himalayan river calcite (Lupker et al., 2012a). The decrease in calcite concentration and Ca/Si ratios since the last glacial maximum supplement the K/Si* and H_2O^+/Si* records, further reinforcing the conclusion that sediment weathering increased during the studied period.

Estuarine and early digenetic reactions such as weathering and reverse weathering may affect the composition of deposited sediments (Jones et al., 2012; Michalopoulos and Aller, 1995, 2004; Wallmann et al., 2008). The close agreement between the chemical composition of modern lower Meghna sediments and the recent part of the record, both from the shelf and the levee, suggests that estuarine processes do not alter significantly the composition of river sediments delivered to the Bay of Bengal. The chemical weathering of sediments after deposition cannot explain the trends observed in the Bay of Bengal record either. Indeed, post-depositional weathering would lead to down-core increase in the weathering intensity which is opposite to the observed trend. Reverse weathering leads to an uptake of K and to an overall decrease in structural OH radicals of the sediments (Michalopoulos and Aller, 1995) but cannot explain the observed down-core increase in detrital carbonate content. Furthermore, during reverse weathering reactions, the newly formed minerals will form in equilibrium with seawater so that the D/H isotopic composition of their hydroxyls groups should become heavier as reverse weathering reactions proceed. However no systematic down-core increase in $\delta D_{H_2O^+}$ is observed (supplementary information, Fig. S1).

5. Sediment provenance since the LGM

Potential sediment source effects on the chemical composition of Bay of Bengal sediments since the LGM must be taken into account as changes in precipitation and erosion patterns within and across the Himalayan range may have affected the sedimentary record. The Sr and Nd isotopic signatures of river sediments in the Himalayan range are a first order indicator of the erosion balance between the Lesser Himalaya (LH) and High Himalaya (HHC) (and Transhimalayan formations – THB – for Brahmaputra)

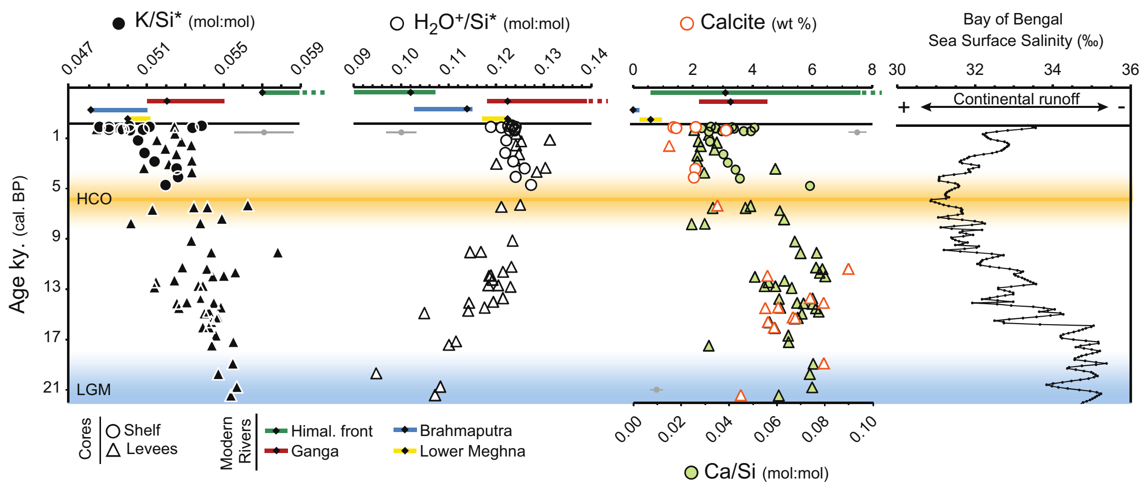

Fig. 6. Evolution of K/Si*, H_2O^+/Si*, Ca/Si and calcite content of sediments in the composite Bay of Bengal record since the last ca. 21 kyr. The composition of river sediments from the modern Himalayan system (average and 1st–3rd quartile range) is also plotted for comparison with the sediment record. The Bay of Bengal sea surface salinity (Kudrass et al., 2001) is shown as a proxy for the Ganga and Brahmaputra continental runoff. The average, 1σ uncertainty on the elemental ratios is indicated by light grey horizontal error bars.

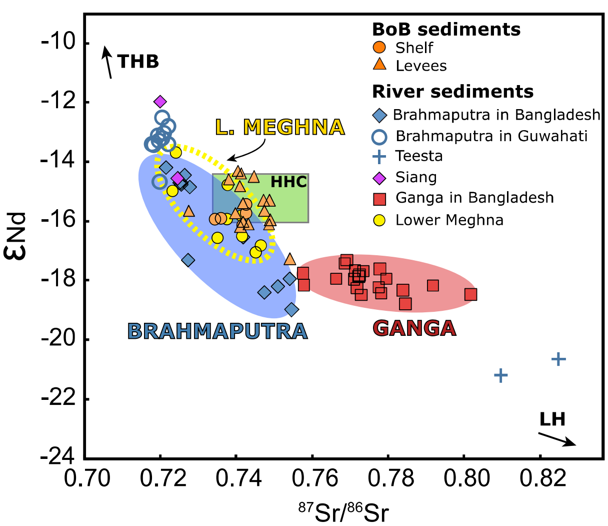

Fig. 7. Sr and Nd isotopic composition of the sediments from the Bay of Bengal. The modern river sediments of the Ganga in Bangladesh, the Brahmaputra in Bangladesh (along with samples from the Siang, the Brahmaputra in Guwahati and the Teesta, Rivers from Singh and France-Lanord, 2002) and the lower Meghna are represented for comparison. The Sr and Nd isotopic data set of the Brahmaputra in Bangladesh has partly been acquired in order to test sediment source effects in the Brahmaputra basin by selecting samples that covered a large span of chemical compositions. This sample choice may have introduced a bias towards samples that recorded a large input from the Teesta upstream right-bank tributary. We therefore suspect the average Sr and Nd isotopic composition of the Brahmaputra to be closer to the Brahmaputra in Guwahati and the Siang than our dataset suggests (see supplementary information). The isotopic composition of the Lesser Himalaya (LH), Higher Himalaya Cristalines (HHC) and Trans Himalayan Batholith (THB) are from Galy and France-Lanord (2001) and references therein.

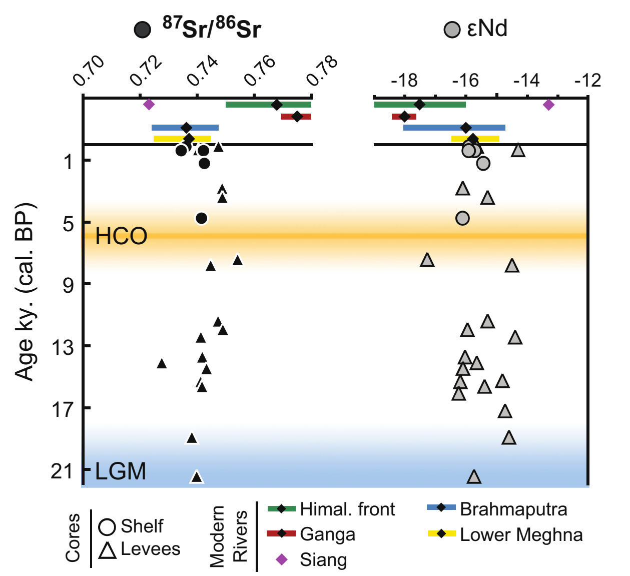

Fig. 8. Sr and Nd isotopic composition of the silicate fraction of Bay of Bengal sediments (Pierson-Wickmann et al., 2001; Galy et al., 2008 and this study) along with the modern river sediments composition of the Himalayan front, the Ganga, the Brahmaputra and the lower Meghna (average and 1st–3rd quartile range). The isotopic composition of sediments from the modern Siang River (Singh and France-Lanord, 2002) is also plotted. The Siang delivers ca. 50% of the sediment load of the Brahmaputra (Singh and France-Lanord, 2002), contributing disproportionally to the final isotopic signature of the modern Brahmaputra.

as these units have contrasted isotopic compositions (France-Lanord et al., 1993; Singh and France-Lanord, 2002). Sediments from the Ganga and Brahmaputra basins also show distinctive Sr and Nd isotopic compositions so that changes in the balance of sediment supply from both basins would be detected (Fig. 7).

Previous studies have shown contrasting changes in the balance between sediments from the LH and HHC in the Indus basin (Clift et al., 2008) and the western part of the Ganga basin (Rahaman et al., 2009, 2010; Srivastava and Shukla, 2010) since deglaciation. However, both Sr and Nd isotopic compositions of Bay of Bengal sediments appear constant, implying that there is no evidence for major changes in the distribution of erosion within the Himalayan range at this scale (Fig. 8). The Sr and Nd record also suggests that the balance between the Brahmaputra and Ganga has remained roughly constant over the last 20 kyrs. A significant change in the sediment balance between Ganga and Brahmaputra would furthermore result in a correlated evolution of K/Si* and H_2O^+/Si*, whereas these ratios are actually anti-correlated since the LGM (Fig. 6), demonstrating that the weathering signal overprints any potential change in sediment source.

An increase in sediments from the Siwalik or from southern tributaries through time is also very unlikely. Siwalik rocks and sediments are characterized by high carbonate content and low $\delta^{13}C$ compositions (Lupker et al., 2012a; Sanyal et al., 2005). Thus, the concomitant decrease of both carbonate content and

$\delta^{13}C$ values observed in the Bay of Bengal sediments is not compatible with an increase of sediment supply from the Siwaliks. In addition, sediments from the Chambal River in the Ganga basin and the Eastern tributaries of the Brahmaputra basin (Lohit and Dibang) have distinctively higher Fe/Si ratios and unradiogenic Sr and Nd signatures (Lupker et al., 2012a; Singh and France-Lanord, 2002; Singh et al., 2008) that are not identified in our record (see supplementary information, Fig. S1).

Altogether, the observed changes in Bay of Bengal sediment mobile elements composition since the LGM can thus be primarily attributed to changes in the chemical weathering intensity in the Ganga and Brahmaputra basin.

6. Discussion

6.1. Climatic forcing of Himalayan chemical weathering

During the last 21 kyrs, climate has been the main external forcing of Himalayan erosion that could have affected the Bay of Bengal weathering signal. Paleo-temperature reconstructions over the Himalayan system are scarce but indicate a ca. 2 °C colder LGM sea surface temperature (SST) in the Bay of Bengal (Kudrass et al., 2001). Hydrological changes were significant with strongly reduced monsoon and therefore a lower continental runoff during the last glacial (Cullen, 1981; Duplessy, 1982; Herzschuh, 2006; Kudrass et al., 2001), which reduced the sediment supply to the Bay of Bengal (Goodbred, 2003; Weber et al., 1997). Precipitation and temperature directly control the weathering rate of minerals (White and Blum, 1995), and the conditions during the LGM where therefore less favorable for intense weathering in the floodplain. These changes in floodplain weathering are confirmed by the evolution of clay assemblages in the southern part of the basin that suggests an increase in weathering intensity from at least 10 kyr to present (Heroy et al., 2003).

Additional, independent processes should not be excluded (Blum and Tornqvist, 2000). The lower base level and a reduced sediment supply during the LGM could have lead to channel incision and a narrower active floodplain (Goodbred, 2003; Heroy et al., 2003), which would reduce channel—floodplain interactions and limit the supply of weathered floodplain sediments to the Bay of Bengal. A complete abandonment of the floodplain during the LGM is nevertheless unlikely as floodplain derived organic material is persistent in the Bay of Bengal cores throughout the deglaciation (Galy et al., 2008) but changes in the sediment locus and volume being mobilized should not be excluded (Dosseto et al., 2010).

The weathering degree of sediments does, however, not show any clear change in response to the decrease of monsoon intensity after the Holocene Climatic Optimum (HCO) (Kudrass et al., 2001). The sediment fluxes during the HCO were up to double modern fluxes as indicated by sediment volume reconstructions (Goodbred, 2003). These high sediment fluxes may have obliterated the intense weathering conditions prevailing at that time. It can also not be ruled out that modern sediments reflect the export of material weathered during the HCO owing to a long-sediment transfer time so that the post-HCO decrease in precipitation is not yet recorded in the Bay of Bengal. The impact of anthropogenic activity in the Indo-Gangetic floodplain should also be considered as intense land use changes, certainly significant more than 3 centuries ago (Ramankutty and Foley, 1999), may overprint the climatic forcing of the weathering degree in the recent part of the record if already significant thousands of years ago (Bayon et al., 2012).

The sediment transfer time through the Himalayan system has to be considered as well, as a long transfer time would induce a temporal offset between the suggested climatic forcing of weathering in the Ganga and Brahmaputra basin and its recording in the sediment record of the Bay of Bengal. The sediment transfer time in large continental basins remains difficult to constrain. U-series disequilibrium studies on Ganga sediments suggest that the transfer time of coarse sediments may reach several 100 kyrs while fine grained suspended material travel in less than 25 kyrs (Chabaux et al., 2006, 2009; Granet et al., 2007, 2010). However, simple mass balance considerations based on the volume of the active floodplain and grain size along with modern sediment fluxes suggest shorter transfer time scales of 1 kyrs for fine (<100 μm) sediments along the Ganga floodplain (Lupker et al., 2012b) and most probably even shorter transfer time along the narrower Brahmaputra floodplain. In addition, short term variability of the chemical composition of Ganga sediments observed in Bangladesh and attributed to the variable input of a >1000 km distant, upstream tributary suggests that for fine-grained suspended sediment the transfer time can be of the order of the season (Lupker et al., 2012a). Finally, a relatively short transfer time is also supported by the organic carbon Bay of Bengal record, which shows a change in vegetation photosynthetic type over the Ganga and Brahmaputra basin from the last glacial to present (Galy et al., 2008). This vegetation change follows the model predictions and would not be recorded if the sediment transfer time exceeded glacial–interglacial time scales.

Although the transfer time of sediments is probably significant and remains difficult to quantify, a network of evidences suggests that it is lower than glacial–interglacial time scales for fine sediments such as those composing the Bay of Bengal record (high Al/Si ratios). Thus, the observed weathering trends most likely results from the direct or indirect climatic forcing of weathering in the Ganga and Brahmaputra basin.

6.2. Towards a quantitative weathering budget

Changes in the net weathering flux or dissolved flux (φ_X) can be estimated by considering that, at steady state, the weathering flux exported as solutes to the oceans is the product of the mobile element depletion of sediments (ΔX) and the sediment flux (F_{sed}) (Lupker et al., 2012a):

$$\varphi_K = F_{sed} \cdot \Delta X = F_{sed} \cdot \left(\frac{\overline{X}}{Si}_{Source} \cdot [\overline{Si}]_{Source} - \frac{\overline{X}}{Si}_{Sink} \cdot [\overline{Si}]_{Sink} \right) \quad (2)$$

where $\overline{X/Si}$ is the average mobile to immobile ratio of the source and sink sediments and $[\overline{Si}]$ the average Si concentration of the sediments. A high-resolution reconstruction of weathering fluxes is pointless, as the steady state hypothesis is likely not fully satisfied over short time-scales because of late Holocene climatic variations and anthropogenic imprints (possibly acting over time-scales shorter than the sediment residence time in the floodplain). A first order estimate can nevertheless be made by comparing the loss of K, and gain in H_2O^+, relative to Himalayan front sediments for the LGM (19–22 kyr) and the modern (0–2 kyr) part of the record.

The average $\overline{K/Si}$ and $\overline{H_2O^+/Si}$ ratios of the exported sediment flux can be estimated based on the average Al/Si ratio of the sediments, as Al/Si is relatively insensitive to chemical weathering. The average Al/Si ratio of sediments was estimated to be 0.23 for the Ganga in Bangladesh (Lupker et al., 2011). Hence, $\overline{K/Si}$ and $\overline{H_2O^+/Si}$ are well approximated by $\overline{K/Si*}$ and $\overline{H_2O^+/Si*}$, as for these ratios the composition of the sediment is normalized to an Al/Si ratio of 0.23.

Because the effect of weathering in the Himalayan range is not detected on the K/Si and H_2O^+/Si composition of modern river sediments sampled at the front of the Himalayan range (Lupker et al., 2012a), we conclude that the composition of these sediments is a good approximation of the average composition of the sediment source. This observation also excludes the possibility of a significantly lower degree of sediment weathering within the Himalayan range during the LGM, as weathering for *K* and H_2O^+ is already limited at present. We therefore consider that the Himalayan front end-member (as constrained from the mixture of 60% of sediments from the Himalayan front in the Brahmaputra basin and 40% in the Ganga basin) is a good first order approximation of the sediment source composition, both in the modern day system and during the LGM. The modern dissolved flux of Si is negligible compared to the solid Si fluxes (Galy and France-Lanord, 2001) and this was most likely also the case during the LGM as the chemical weathering intensity was even lower than at present. Furthermore the Si concentration of the exported sediments is only slightly affected by sequestration of Si-rich bedload sediments in the modern floodplain (Lupker et al., 2012a) and we make the assumption that this has been true during the last 21 kyrs. Hence, we consider $[\overline{Si}]$ constant during the time span of our record.

The change in the weathering flux ($R\varphi_X$) of mobile element *X* from LGM to present relative to the modern fluxes can therefore be written as:

$$R\varphi_X = \frac{\varphi_X|_{Modern} - \varphi_X|_{LGM}}{\varphi_X|_{Modern}} = \frac{F_{Sed}^{Modern}\cdot\left(X/Si^*|_{Himal\ Front}^{Modern} - X/Si^*|_{BoB}^{Modern}\right) - F_{Sed}^{LGM}\cdot\left(X/Si^*|_{Himal\ Front}^{LGM} - X/Si^*|_{BoB}^{LGM}\right)}{F_{Sed}^{Modern}\cdot\left(X/Si^*|_{Himal\ Front}^{Modern} - X/Si^*|_{BoB}^{Modern}\right)} \quad (3)$$

In order to estimate $R\varphi_X$ from Eq. (3), the sediment flux (F_{sed}) has to be estimated at present and during the LGM. Based on extensive gauging data the combined modern flux of the Ganga and Brahmaputra in Bangladesh is estimated to be ca. 1×10^9 t yr^{-1} (RSP, 1996). The past sediment flux exported by the Ganga and Brahmaputra is largely unknown. However, qualitatively, the sediment flux was most probably lower during the LGM than at present. A weakened monsoon during the LGM (Kudrass et al., 2001; Sharma et al., 2004) may have limited physical erosion in the Himalayan range and lowered the transport capacity of the rivers, leading to a lower sediment flux to the Bay of Bengal (Weber et al., 1997; Goodbred, 2003). A very conservative estimate of the minimum value of $R\varphi_X$ can therefore be made assuming a constant sediment flux over the period. By doing so we also isolate the effect of the change in the chemical composition of sediments only.

$R\varphi$ was computed using Eq. (3) for *K* and H_2O^+ and is summarized in Table 1. Uncertainties on the K/Si* and H_2O^+/Si* ratios of individual samples are ca. 3% (Supplementary information S3). This is of the same order as the variability of K/Si* and H_2O^+/Si* ratios over the 0–2 and 19–22 kyr intervals or of the uncertainties on the regression through the data for the Himalayan front sediments. These uncertainties were propagated through the calculations of $R\varphi_X$ and reported in Table 1. The sensitivity of the weathering budget to the average Al/Si ratio of sediments is lower than the uncertainty propagated from the variability of K/Si* and H_2O^+/Si* ratios (see supplementary information S3). This first order estimation shows that the weathering flux during the LGM was at least 67 ($\pm$28)% and 89 ($\pm$36)% lower (for *K* and H_2O^+, respectively) than for the modern period (0–2 kyrs) for a constant sediment flux (i.e. respectively 33% and 11% of the present weathering flux). The main uncertainty on these estimates comes from the uncertainty on the sediment Ganga and Brahmaputra sediment flux during the LGM. A sediment flux during the LGM of half the present day sediment flux would induce a 83% and 95% lower weathering flux during the LGM compared to present for *K* and H_2O^+, respectively (i.e. 17% and 5% of the present weathering flux).

Table 1
Relative changes in the weathering flux delivered to the Bay of Bengal as dissolved load from the LGM to present ($R\varphi_K$ and $R\varphi_{H_2O^+}$) assuming a constant sediment flux over the period. The weathering flux was estimated using Eq. (3) for *K* and H_2O^+ from the Himalayan front and Bay of Bengal end-members reported in the table.

		LGM	Modern
Sediment flux (t/yr)		1×10^9	1×10^9
Himalayan front	$\overline{K/Si^*}$	0.0574 ($\pm$0.0025)	0.0574 ($\pm$0.0025)
	$\overline{H_2O^+/Si^*}$	0.1009 ($\pm$0.0068)	0.1009 ($\pm$0.0068)
Bay of Bengal	$\overline{K/Si^*}$	0.0553 ($\pm$0.0005)	0.0510 ($\pm$0.0017)
	$\overline{H_2O^+/Si^*}$	0.1034 ($\pm$0.0075)	0.1236 ($\pm$0.0026)
	$\boldsymbol{R\varphi_K}$	67 ($\pm$28)%	
	$\boldsymbol{R\varphi_{H_2O^+}}$	89 ($\pm$36)%	

The loss of *K* in the Himalayan system is mainly attributed to the weathering of biotite while the gain in hydration also depends on clay secondary mineral formation (Lupker et al., 2012a). Because the reaction mechanisms in both cases are different, their sensitivity to changes in precipitation and temperature is also most probably different. Despite our estimates for both proxies being similar within uncertainty, it would not be surprising that the relative changes in weathering fluxes recorded by *K* and H_2O^+ could be different. It is not possible to estimate the relative change in calcite weathering using a similar approach, because for calcite the Himalayan source composition cannot be reliably estimated. Indeed, significant carbonate dissolution has been documented within the Himalayan range (Galy et al., 1999), hence, Himalayan front river sediments cannot accurately represent the eroded source. In addition, no direct estimation of the average calcite content of Himalayan rocks is available.

Our quantification of the change in the net weathering flux from LGM to present should only be considered as a rough estimate. In particular, it should be kept in mind that these estimates somewhat depend upon the assumption of a transition between two steady state weathering stages. Nevertheless, our estimates suggest that changes in weathering fluxes exported by the Himalayan system have been significant over short time scales of ca. 20 kyrs. The magnitude of the variations in weathering fluxes reconstructed here exceeds previous estimates (Foster and Vance, 2006). This may be attributed in part to the very high weathering rates of glacial outwash during the very early stage of an interglacial, as proposed earlier (Foster and Vance, 2006; Vance et al., 2009) combined to the short time span of our record. However, for the Himalayan system the weathering intensity in the modern floodplain (Lupker et al., 2012a; West et al., 2002) supports the dominant role of the floodplain in modulating glacial to interglacial weathering fluxes. This study further emphasizes that present day weathering rates are likely higher than long-term averages, which supports the idea that the imbalance of oceanic geochemical cycles may at least partially derive from the over-estimation of Quaternary riverine fluxes to the oceans (Vance et al., 2009).

7. Conclusions

The geochemistry of detrital sediment records holds valuable information on the weathering regime these sediments have undergone during their transit from sediment producing areas to their deposition in sedimentary basins. The chemical composition of these sediments is primarily controlled by sediment sorting effects that occur during transport and deposition. Nevertheless weathering signals can be extracted from the sediment chemical composition if sorting is properly taken into account by comparing sediment records to modern river systems.

The detrital record presented here shows that the degree of chemical weathering experienced by sediments exported by the Himalayan system, drained by the Ganga and Brahmaputra Rivers, has changed significantly since the LGM. An overall decrease in potassium and detrital calcite content along with an increase in sediment hydration all point towards a steady increase in the weathering degree of sediments over the last 21 kyrs, while the sediment provenance has remained unchanged. These changes in the weathering regime are attributed to the direct climatic forcing of chemical weathering in the floodplain, as increasing precipitation and temperatures after the deglaciation favored mineral weathering kinetics. Additional hydrological changes in response to increasing runoff and rising base level might also have impacted weathering through enhanced channel-floodplain interactions.

A first order estimation of changes in the weathering flux delivered to the oceans can be made using the detrital record and conservatively assuming a steady sediment flux. It shows that weathering fluxes from the Himalayan system could have been reduced by 90% during the LGM. This supports previous evidence that current dissolved fluxes are likely higher than average Quaternary estimates. These drastic changes in solute supply to the oceans on glacial–interglacial time scales have to be accounted for to reconstruct global oceanic biogeochemical cycles.

Acknowledgments

This work was supported by French INSU program ‘‘Relief de la Terre’’ and ANR Calimero. V.G. was supported by the US National Science Foundation (Grants OCE-0851015and OCE-0928582). We thank C. Guilmette for assistance in the lab. H. Schopka and two anonymous reviewers are also thanked for their constructive comments that helped to improve the manuscript. T.M. Harrison is acknowledged for the very efficient handling of the manuscript.

Appendix A. Supporting information

Supplementary data associated with this article can be found in the online version at http://dx.doi.org/10.1016/j.epsl.2013.01.038.

References

Bayon, G., Dennielou, B., Etoubleau, J., Ponzevera, E., Toucanne, S., Bermell, S., 2012. Intensifying weathering and land use in Iron Age Central Africa. Science 335, 1219–1222, http://dx.doi.org/10.1126/science.1215400.

Blum, M.D., Tornqvist, T.E., 2000. Fluvial responses to climate and sea-level change: a review and look forward. Sedimentology 47, 2–48.

Bouchez, J., Gaillardet, J., France-Lanord, C., Maurice, L., Dutra-Maia, P., 2011a. Grain size control of river suspended sediment geochemistry: clues from Amazon River depth profiles. Geochem. Geophys. Geosyst. 12, Q03008, http://dx.doi.org/10.1029/2010gc003380.

Bouchez, J., Lupker, M., Gaillardet, J., France-Lanord, C., Maurice, L., 2011b. How important is it to integrate riverine suspended sediment chemical composition with depth? Clues from Amazon River depth-profiles. Geochim. Cosmochim. Acta 75, 6955–6970, http://dx.doi.org/10.1016/j.gca.2011.08.038.

Carignan, J., Hild, P., Mevelle, G., Morel, J., Yeghicheyan, D., 2001. Routine analyses of trace elements in geological samples using flow injection and low pressure on-line liquid chromatography coupled to ICP-MS: a study of geochemical reference materials BR, DR-N, UB-N, AN-G and GH. Geostand. Newsl. J. Geostand. Geoanal. 25, 187–198.

Chabaux, F., Granet, M., Blaes, E., Dosseto, A., France-Lanord, C., Valier, V., 2009. Determination of source and transfer-time of river sediments in alluvial plain from U-series nuclides: evidence from the Ganges River System. Geochim. Cosmochim. Acta 73, A203, A203.

Chabaux, F., Granet, M., France-Lanord, C., Stille, P., 2006. U-series in Himalayan rivers: timescale of sedimentary transfer. Geochim. Cosmochim. Acta 70, A92, http://dx.doi.org/10.1016/j.gca.2006.06.097 ISSN: 0016-7037.

Clift, P.D., Giosan, L., Biusztajn, J., Campbell, I.H., Allen, C., Pringle, M., Tabrez, A.R., Danish, M., Rabbani, M.M., Alizai, A., Carter, A., Lueckge, A., 2008. Holocene erosion of the Lesser Himalaya triggered by intensified summer monsoon. Geology 36, 79–82, http://dx.doi.org/10.1130/g24315a.1 ISSN: 0091-7613.

Cullen, J.L., 1981. Microfossil evidence for changing salinity patterns in the Bay of Bengal over the last 20000 years. Palaeogeogr. Palaeoclim. Palaeoecol. 35, 315–356.

Dosseto, A., Hesse, P.P., Maher, K., Fryirs, K., Turner, S., 2010. Climatic and vegetation control on sediment dynamics during the last glacial cycle. Geology 38, 395–398, http://dx.doi.org/10.1130/g30708.1.

Duplessy, J.C., 1982. Glacial to interglacial contrasts in the northern Indian Ocean. Nature 295, 494–498.

Foster, G.L., Vance, D., 2006. Negligible glacial–interglacial variation in continental chemical weathering rates. Nature 444, 918–921, http://dx.doi.org/10.1038/nature05365.

France-Lanord, C., Derry, L., 1997. Organic carbon burial forcing of the carbon cycle from Himalayan erosion. Nature 390, 65–66.

France-Lanord, C., Derry, L., Michard, A., 1993. Evolution of the Himalaya since Miocene time: isotopic and sedimentologic evidence from the Bengal Fan. In: Treloar, P.J., Searle, M. (Eds.), Himalayan Tectonics. Geological Society of London, London, pp. 603–621.

Galy, A., France-Lanord, C., 2001. Higher erosion rates in the Himalaya: geochemical constraints on riverine fluxes. Geology 29, 23–26.

Galy, A., France-Lanord, C., Derry, L.A., 1999. The strontium isotopic budget of Himalayan Rivers in Nepal and Bangladesh. Geochim. Cosmochim. Acta 63, 1905–1925.

Galy, V., François, L., France-Lanord, C., Faure, P., Kudrass, H., Palhol, F., Singh, S., 2008. C4 plants decline in the Himalayan basin since the Last Glacial Maximum. Quat. Sci. Rev. 27, 1396–1409, http://dx.doi.org/10.1016/j.quascirev.2008.04.005.

Garzanti, E., Ando, S., France-Lanord, C., Censi, P., Vignola, P., Galy, V., Lupker, M., 2011. Mineralogical and chemical variability of fluvial sediments 2. Suspended-load silt (Ganga–Brahmaputra, Bangladesh). Earth Planet. Sci. Lett. 302, 107–120, http://dx.doi.org/10.1016/j.epsl.2010.11.043.

Garzanti, E., Ando, S., France-Lanord, C., Vezzoli, G., Censi, P., Galy, V., Najman, Y., 2010. Mineralogical and chemical variability of fluvial sediments 1. Bedload sand (Ganga-Brahmaputra, Bangladesh). Earth Planet. Sci. Lett. 299, 368–381, http://dx.doi.org/10.1016/j.epsl.2010.09.017.

Goodbred, S.L., 2003. Response of the Ganges dispersal system to climate change: a source-to-sink view since the last interstade. Sediment. Geol. 162, 83–104.

Granet, M., Chabaux, F., Stille, P., Dosseto, A., France-Lanord, C., Blaes, E., 2010. U-series disequilibria in suspended river sediments and implication for sediment transfer time in alluvial plains: the case of the Himalayan rivers. Geochim. Cosmochim. Acta 74, 2851–2865, http://dx.doi.org/10.1016/j.gca.2010.02.016.

Granet, M., Chabaux, F., Stille, P., France-Lanord, C., Pelt, E., 2007. Time-scales of sedimentary transfer and weathering processes from U-series nuclides: clues from the Himalayan rivers. Earth Planet. Sci. Lett. 261, 389–406, http://dx.doi.org/10.1016/j.epsl.2007.07.012 ISSN: 0012-821X.

Heroy, D., Kuehl, S., Goodbred, S., 2003. Mineralogy of the Ganges and Brahmaputra rivers: implications for river switching and Late Quaternary climate change. Sediment. Geol. 155, 343–359.

Herzschuh, U., 2006. Palaeo-moisture evolution in monsoonal Central Asia during the last 50,000 years. Quat. Sci. Rev. 25, 163–178.

Hoehndorf, A., Kudrass, H.R., France-Lanord, C., 2003. Transfer of the Sr isotopic signature of the Himalayas to the Bay of Bengal. Deep Sea Res. Part II-Top. Stud. Oceanogr. 50, 951–960, http://dx.doi.org/10.1016/s0967-0645(02)00614-8 ISSN: 0967-0645.

Ittekkot, V., Kudrass, H.R., Quadfasel, D., Unger, D., 2003. The Bay of Bengal—an introduction. Deep Sea Res. Part II: Top. Stud. Oceanogr. 50, 853–854.

Jones, M.T., Pearce, C.R., Oelkers, E.H., 2012. An experimental study of the interaction of basaltic riverine particulate material and seawater. Geochim. Cosmochim. Acta 77, 108–120, http://dx.doi.org/10.1016/j.gca.2011.10.044.

Kudrass, H., Hofmann, A., Doose, H., Emeis, K., Erlenkeuser, H., 2001. Modulation and amplification of climatic changes in the Northern Hemisphere by the Indian summer monsoon during the past 80 k.y. Geology 29, 63–66.

Limmer, D.R., Böning, P., Giosan, L., Ponton, C., Köhler, C.M., Cooper, M.J., Tabrez, A.R., Clift, P.D., 2012. Geochemical record of Holocene to Recent sedimentation on the Western Indus continental shelf, Arabian Sea. Geochem. Geophys. Geosyst. 13, Q01008, http://dx.doi.org/10.1029/2011gc003845.

Lupker, M., France-Lanord, C., Galy, V., Lavé, J., Gaillardet, J., Gajurel, A.P., Guilmette, C., Rahman, M., Singh, S.K., Sinha, R., 2012a. Predominant floodplain over mountain weathering of Himalayan sediments (Ganga basin). Geochim. Cosmochim. Acta 84, 410–432, http://dx.doi.org/10.1016/j.gca.2012.02.001.

Lupker, M., Blard, P.-H., Lavé, J., France-Lanord, C., Leanni, L., Puchol, N., Charreau, J., Bourlès, D., 2012b. ^{10}Be-derived Himalayan denudation rates and sediment budgets in the Ganga basin. Earth Planet. Sci. Lett. 333–334, 146–156, http://dx.doi.org/10.1016/j.epsl.2012.04.020.

Lupker, M., France-Lanord, C., Lavé, J., Bouchez, J., Galy, V., Métivier, F., Gaillardet, J., Lartiges, B., Mugnier, J.-L., 2011. A Rouse-based method to integrate the

chemical composition of river sediments: application to the Ganga basin. J. Geophys. Res. 116, F04012, http://dx.doi.org/10.1029/2010jf001947.
Michalopoulos, P., Aller, R.C., 1995. Rapid clay mineral formation in Amazon Delta sediments: reverse weathering and oceanic elemental cycles. Science 270, 614.
Michalopoulos, P., Aller, R.C., 2004. Early diagenesis of biogenic silica in the Amazon delta: alteration, authigenic clay formation, and storage. Geochim. Cosmochim. Acta 68, 1061–1085, http://dx.doi.org/10.1016/j.gca.2003.07.018.
Michels, K.H., Kudrass, H.R., H. bscher, C., Suckow, A., Wiedicke, M., 1998. The submarine delta of the Ganges–Brahmaputra: cyclone-dominated sedimentation patterns. Mar. Geol. 149, 133–154.
Pierson-Wickmann, A.-C., Reisberg, L., France-Lanord, C., Kudrass, H., 2001. Os–Sr–Nd results from sediments in the Bay of Bengal: implications for sediment transport and the marine Os record. Paleoceanography 16, 435–444.
Rahaman, W., Singh, S.K., Sinha, R., Tandon, S.K., 2009. Climate control on erosion distribution over the Himalaya during the past ~100 ka. Geology 37, 559–562, http://dx.doi.org/10.1130/g25425a.1.
Rahaman, W., Singh, S.K., Sinha, R., Tandon, S.K., 2010. Climate control on erosion distribution over the Himalaya during the past similar to 100 ka: REPLY. Geology 38, E217, http://dx.doi.org/10.1130/g31119y.1, E217.
Ramankutty, N., Foley, J.A., 1999. Estimating historical changes in global land cover: croplands from 1700 to 1992. Global Biogeochem. Cycles 13, 997–1027, http://dx.doi.org/10.1029/1999gb900046.
Raymo, M., Ruddiman, W., Froelich, P., 1988. Influence of late Cenozoic mountain building on ocean geochemical cycles. Geology 16, 649.
Reimer, P.J., Baillie, M.G.L., Bard, E., Bayliss, A., Beck, J.W., Blackwell, P.G., Ramsey, C.B., Buck, C.E., Burr, G.S., Edwards, R.L., Friedrich, M., Grootes, P.M., Guilderson, T.P., Hajdas, I., Heaton, T.J., Hogg, A.G., Hughen, K.A., Kaiser, K.F., Kromer, B., McCormac, F.G., Manning, S.W., Reimer, R.W., Richards, D.A., Southon, J.R., Talamo, S., Turney, C.S.M., van der Plicht, J., Weyhenmeye, C.E., 2009. Intcal09 and Marine09 Radiocarbon Age calibration curves, 0–50,000 years Cal Bp. Radiocarbon 51, 1111–1150.
RSP, 1996. River Survey Project, Flood Action Plan (FAP) final report. Delft Hydraulics and DHI.
Sanyal, P., Bhattacharya, S.K., Prasad, M., 2005. Chemical diagenesis of Siwalik sandstone: isotopic and mineralogical proxies from Surai Khola section, Nepal. Sediment. Geol. 180, 57–74.
Sharma, S., Joachimski, M., Sharma, M., Tobschall, H.J., Singh, I.B., Sharma, C., Chauhan, M.S., Morgenroth, G., 2004. Lateglacial and Holocene environmental changes in Ganga plain, Northern India. Quat. Sci. Rev. 23, 145–159.
Singh, S., France-Lanord, C., 2002. Tracing the distribution of erosion in the Brahmaputra watershed from isotopic compositions of stream sediments. Earth Planet. Sci. Lett. 252, 645–662.
Singh, S.K., Rai, S.K., Krishnaswami, S., 2008. Sr and Nd isotopes in river sediments from the Ganga Basin: sediment provenance and spatial variability in physical erosion. J. Geophys. Res. 113, F03006, http://dx.doi.org/10.1029/2007jf000909.
Singh, S.K., Sarin, M.M., France-Lanord, C., 2005. Chemical erosion in the eastern Himalaya: major ion composition of the Brahmaputra and delta C-13 of dissolved inorganic carbon. Geochim. Cosmochim. Acta 69, 3573–3588, http://dx.doi.org/10.1016/j.gca.2005.02.033|ISSN 0016-7037.
Srivastava, P., Shukla, U.K., 2010. Climate control on erosion distribution over the Himalaya during past similar to 100 ka: COMMENT. Geology 38, E216, http://dx.doi.org/10.1130/g30838c.1, E216.
Vance, D., Teagle, D.A.H., Foster, G.L., 2009. Variable quaternary chemical weathering fluxes and imbalances in marine geochemical budgets. Nature 458, 493–496, http://dx.doi.org/10.1038/nature07828.
Walker, J., Hays, P., Kasting, J., 1981. A negative feedback mechanism for the long-term stabilization of the Earth's surface temperature. J. Geophys. Res. 86, 9776–9782.
Wallmann, K., Aloisi, G., Haeckel, M., Tishchenko, P., Pavlova, G., Greinert, J., Kutterolf, S., Eisenhauer, A., 2008. Silicate weathering in anoxic marine sediments. Geochim. Cosmochim. Acta 72, 2895–2918.
Weber, M.E., Wiedicke, M.H., Kudrass, H.R., Hübscher, C., Erlenkeuser, H., 1997. Active growth of the bengal Fan during sea-level rise and highstand. Geology 25, 315–318.
West, A.J., Bickle, M.J., Collins, R., Brasington, J., 2002. Small-catchment perspective on Himalayan weathering fluxes. Geology 30, 355–358, http://dx.doi.org/10.1130/0091-7613(2002)030 < 0355:scpohw > 2.0.co;2.
White, A.F., Blum, A.E., 1995. Effects of climate on chemical weathering in watersheds. Geochim. Cosmochim. Acta 59.
Willenbring, J.K., von Blanckenburg, F., 2011. Long-term stability of global erosion rates and weathering during late-Cenozoic cooling. Nature 465, 211–214, http://dx.doi.org/10.1038/nature09044.